Journal of
Plankton Research

plankt.oxfordjournals.org

J. Plankton Res. (2016) 38(2): 256–270. First published online January 13, 2016 doi:10.1093/plankt/fbv109

Costa Rica Dome: Flux and Zinc Experiments

Microplankton trace element contents: implications for mineral limitation of mesozooplankton in an HNLC area

STEPHEN B. BAINES[1]*, XI CHEN[2], STEFAN VOGT[3], NICHOLAS S. FISHER[2], BENJAMIN S. TWINING[4] AND MICHAEL R. LANDRY[5]

[1]DEPARTMENT OF ECOLOGY AND EVOLUTION, STONY BROOK UNIVERSITY, STONY BROOK, NY 11789-5245, USA, [2]SCHOOL OF MARINE AND ATMOSPHERIC SCIENCES, STONY BROOK UNIVERSITY, STONY BROOK, NY 11789-5000, USA, [3]ADVANCED PHOTON SOURCE, ARGONNE NATIONAL LABORATORY, ARGONNE, IL 60439, USA, [4]BIGELOW LABORATORY OF OCEAN SCIENCES, EAST BOOTHBAY, ME 04544, USA AND [5]SCRIPPS INSTITUTION OF OCEANOGRAPHY, UNIVERSITY OF CALIFORNIA AT SAN DIEGO, 9500 GILMAN DR, LA JOLLA, CA 92093-0227, USA

*CORRESPONDING AUTHOR: stephen.baines@stonybrook.edu

Received June 6, 2015; accepted November 19, 2015

Corresponding editor: John Dolan

Mesozooplankton production in high-nutrient low-chlorophyll regions of the ocean may be reduced if the trace element concentrations in their food are insufficient to meet growth and metabolic demands. We used elemental microanalysis (SXRF) of single-celled plankton to determine their trace metal contents during a series of semi-Lagrangian drift studies in an HNLC upwelling region, the Costa Rica Dome (CRD). Cells from the surface mixed layer had lower Fe:S but higher Zn:S and Ni:S than those from the subsurface chlorophyll maximum at 22–30 m. Diatom Fe:S values were typically 3-fold higher than those in flagellated cells. The ratios of Zn:C in flagellates and diatoms were generally similar to each other, and to co-occurring mesozooplankton. Estimated Fe:C ratios in flagellates were lower than those in co-occurring mesozooplankton, sometimes by more than 3-fold. In contrast, Fe:C in diatoms was typically similar to that in zooplankton. RNA:DNA ratios in the CRD were low compared with other regions, and were related to total autotrophic biomass and weakly to the discrepancy between Zn:C in flagellated cells and mesozooplankton tissues. Mesozooplankton may have been affected by the trace element content of their food, even though trace metal limitation of phytoplankton was modest at best.

KEYWORDS: mineral limitation; diatoms; flagellates; mesozooplankton; zinc; iron; nickel; manganese; trace metals; SXRF

available online at www.plankt.oxfordjournals.org

INTRODUCTION

While mesozooplankton growth and reproduction is usually presumed to reflect food availability (Bottrell *et al.*, 1976; Hirst and Bunker, 2003), food quality can also be a limiting factor. The elemental composition of food is one factor that affects its quality. Many crustaceans exhibit little variability in the nitrogen and phosphorus contents of their tissues and so must obtain required amounts of N and P from their diet to produce more biomass (Hessen, 1992). When the concentration of these nutrient elements in the diet is low, crustacean production may become a function of the N:C and P:C of the food, rather than of the amount of food in the environment (Hessen, 1992; Sterner and Hessen, 1994; Elser and Urabe, 1999). Such limitations may be particularly acute for younger life stages (Villar-Argaiz and Sterner, 2002), and impact growth and reproduction, as observed extensively in freshwater zooplankton feeding on low-P food (Sterner and Elser, 2002). Laboratory experiments suggest that both N- and P-limitation of egg production and somatic growth may occur in marine copepods as well (Kiørboe, 1989; Jones *et al.*, 2002; Malzahn *et al.*, 2010; Malzahn and Boersma, 2012). However, comparisons of C:N and C:P ratios between adult marine mesozooplankton and seston indicate that marine systems may exhibit mineral limitation less frequently and less severely than freshwater systems (Hessen, 1992; Elser and Hassett, 1994) and physiological models differ in whether N-limitation is likely or not (Anderson and Hessen, 1995; Kuijper et al., 2004).

Widespread mineral limitation of marine mesozooplankton production by iron would seem likely for a number of reasons. Like N and P, Fe is a required element used in proteins of the respiratory electron transport system (Raven *et al.*, 1999), as well as in a wide variety of other enzymes (Fraústo Da Silva and Williams, 2001). Fe is nearly insoluble in seawater and is often depleted relative to N and P in deep upwelling water. Phytoplankton Fe content can be extremely variable, ranging over 3 orders of magnitude in response to ambient free Fe^{3+} (Sunda and Huntsman, 1997). Given the same ambient Fe concentrations, different species of phytoplankton can vary in their Fe contents by an order of magnitude (Twining and Baines, 2013). Among other things, such differences reflect variability in allocation to different photosynthetic enzymes (Strzepek and Harrison, 2004) and the presence of storage enzymes (Marchetti *et al.*, 2009). Primary production in up to 40% of the world's oceans is estimated to be periodically subject to iron limitation, potentially causing widespread variability in Fe contents of phytoplankton (Aumont *et al.*, 2003; Moore *et al.*, 2004). Phytoplankton in such regions have cellular Fe:C ratios well below those typical of zooplankton, and *Acartia tonsa*-fed Fe-depleted food exhibited reduced egg production and higher naupliar mortality (Chen *et al.*, 2011).

Although more soluble in seawater than iron, zinc could also act as a limiting factor for mesozooplankton. Zinc is often a structural element within finger motifs of proteins involved in gene regulation, translation and DNA repair, and also functions as a Lewis acid in biochemical reactions (Fraústo Da Silva and Williams, 2001). Like Fe, Zn contents of cultured algae vary with available Zn concentrations (Sunda and Huntsman, 1992). Zn:P also varies among types of phytoplankton, being relatively low in cyanobacteria and relatively high in diatoms (Twining *et al.*, 2004, 2011). Clear evidence of zinc limitation of phytoplankton production has proven difficult to obtain. Nonetheless, Zn:C ratios measured in protists from the eastern equatorial Pacific (EEP) (10–16 μmol mol^{-1}; Twining *et al.*, 2011) are 4-fold lower than the median mesozooplankton Zn:C values reported by a number previous studies (66 μmol mol^{-1}; Baines *et al.*, 2016), suggesting that dietary Zn could limit mesozooplankton production in this region.

In this paper, we determine if Fe and Zn contents of single-celled plankton are low enough to cause Fe and Zn limitation of mesozooplankton in the Costa Rica Dome (CRD). The CRD is a region with an extremely shallow (10–20 m) mixed layer (ML) caused by Ekman pumping of deep water toward the surface. Although relatively productive, it is typically characterized by micromolar concentrations of nitrate and >0.1 μmol L^{-1} phosphate in surface waters (Broenkow, 1965; Fiedler, 2002; Ahlgren *et al.*, 2014), and is therefore among the ocean areas originally classified as high-nutrient low-chlorophyll regions (Minas *et al.*, 1986). Mesoscale Fe addition experiments have not been conducted in the CRD, but ambient Fe concentrations are low, suggesting that Fe could be limiting to primary production (Franck *et al.*, 2005). Shipboard experiments indicate possible roles for both Fe and Zn, and possibly Co, in limitation of phytoplankton growth (Franck *et al.*, 2003, 2005; Saito *et al.*, 2005). Also, the CRD is one of the few ocean regions where the solitary cyanobacterium, *Synechococcus*, dominates the phytoplankton and achieves bloom-like densities (Saito *et al.*, 2005). Whereas eukaryote phytoplankton appear to be limited by Zn in the CRD (Franck *et al.*, 2003), the low Zn quotas and high supply rates of Co seem to favor *Synechococcus* (Saito *et al.*, 2005; Ahlgren *et al.*, 2014).

As part of the CRD FLUx and Zinc Experiments (FLUZiE) project, we measured Zn and Fe contents of single-celled plankton in the CRD in 2010 to determine if concentrations of Fe and Zn might limit secondary production. Measurements were conducted on cells

collected during five Lagrangian process studies, some initiated within the CRD and others outside or on the edge of the feature (Landry *et al.*, 2016a). To determine if there was vertical heterogeneity in the trace element contents of single-celled plankton, we analyzed cells from both the surface ML and from the subsurface chlorophyll maximum (SSCM). Using the resulting data, we compare elemental contents of flagellates and diatoms to determine if these organisms differed in terms of their quality as food for metazoans, and if they possessed unique elemental signatures (Mn and Ni contents) that could be used to trace their importance as food sources. We then compare Fe and Zn in cells with elemental requirements of mesozooplankton. Finally, we assess whether RNA:DNA ratios measured in bulk size fractions of the mesozooplankton community indicate relative low growth and whether these ratios correlate to Fe or Zn contents of phytoplankton.

METHOD

Sampling and sample preparation

Samples for cell elemental analyses were collected as part of a larger project looking at the roles of Fe, Zn and Si in shaping phytoplankton communities and biogeochemical processes in the CRD conducted on R/V Melville cruise MV1008 (22 June–25 July 2010). The data presented here come from five separate semi-Lagrangian drift cycles. Each cycle tracked variation in plankton biomass and growth, nutrient levels and key biogeochemical processes over 4 days using a satellite-tracked drifter drogued at 15 m (Landry *et al.*, 2016a). Samples for single-cell elemental analysis were collected using a trace metal clean rosette with eight 5 L Teflon®-coated exterior spring Niskin-type bottles (Ocean Test Equipment) suspended on a plastic-sheathed wire (Chappell *et al.*, 2016). To address possible vertical heterogeneity in species composition and cellular trace element contents, we sampled both the surface ML and the SSCM. Owing to the shallow mixed layers encountered, ML samples were taken from as deep as possible to avoid contamination from the ship (10–15 m). SSCM depth was determined from profiles of *in vivo* chlorophyll fluorescence. Samples were taken at two points during each cycle, but not all samples were analyzed for elemental contents.

After sampling, the Niskin bottles were carried to a trace metal clean van with class 100 HEPA filtered air (Chappell *et al.*, 2016). Samples were prepared for single-cell elemental analysis by sedimenting cells onto gold transmission electron microscopy grids that were coated with carbon-formvar (Twining *et al.*, 2004, 2011). All manipulations were done in a laminar flow hood and all materials and media were cleaned of trace metals. Whole grids were imaged at sea under 200× magnification using a Zeiss Axiovert 200 M inverted epifluorescence microscope with a 182 Zeiss AxioCam HRc color CCD digital camera and epifluorescence filter sets for detection of chlorophyll *a*, phycoerythrin and FITC. The latter filter set detects fluorescence from the glutaraldehyde fixative, which distinguished organic and inorganic material. Chlorophyll fluorescence was used to identify photosynthetic cells and phycoerythrin fluorescence was used to identify cyanobacterial cells. Diatom and flagellated cells were distinguished by their morphology using differential interference contrast images.

Synchrotron x-ray fluorescence microscopy

Elemental contents of single cells were determined using synchrotron x-ray fluorescence microscopy (SXRF) (Twining *et al.*, 2003). Analyses were conducted at the 2-ID-E beamline of the Advanced Photon Source at Argonne National lab in Argonne, IL, USA. Energy of the incident beam was 10 keV, and the focused spot size ranged between 0.3 and 0.7 μm. Samples were moved stepwise in raster fashion relative to the fixed focused beam, and x-ray fluorescence emissions ranging from 1 to 10 keV were collected at each point using either an energy dispersive Ge detector or a four-element energy dispersive Si(Li) detector. Step sizes were kept below this spatial resolution to ensure that cells were fully sampled by the incident beam. We adjusted the time spent collecting fluorescence spectra at each scan position to obtain 10% counting precision for iron and zinc in the cell as a whole. Spectra were summed for a region encompassing the cell, and for a nearby background region. Counts associated with emission peaks were estimated by fitting the spectra for the cell and background separately to a summed exponentially modified Gaussian model in the program MAPS (Vogt, 2003). Areas were converted to elemental concentrations by comparison with two sets of thin-film standards (NBS-1832 and NBS-1833) made specifically for x-ray fluorescence by the National Bureau of Standards, Gaithersburg Maryland, USA (National Bureau of Standards reference therein). The fluorescence yield for elements not included in the standards, including S and P, was estimated by interpolation using the regression of observed against theoretical fluorescence yields for elements in the standard (Nunez-Milland *et al.*, 2010). Only elemental contents for which the peak area from the spectral fitting procedure was five times greater than the parameter estimation errors are reported.

Within each cell type, we tried to analyze cells representing a range of sizes and taxa so as to encompass the full range of variability in elemental content among cells. In addition to Fe and Zn, we report on cellular Ni and

Mn as these elements are often enriched in diatoms and autotrophs, respectively (Twining and Baines, 2013), making their concentrations in zooplankton possible tracers of these cell types as dietary sources of Fe and Zn. Cellular Mn and Ni may also exhibit variation with depth, because these elements are tied to photosynthesis and uptake of recycled urea, respectively. If such variation with depth exists, concentrations of these elements in mesozooplankton tissues could indicate whether they preferentially feed at depth or in surface waters.

We also report on cellular S, which as a component of cysteine is a proxy for cell protein and carbon (Twining *et al.*, 2003, 2004, 2011). While cellular S can be elevated in living cells due to accumulation of DMS (Sunda *et al.*, 2002), we rarely see such elevated S concentrations in dried cells, possibly because DMS diffuses out of the cell during fixation or volatilizes from cells during drying. All patterns in elemental composition of plankton are analyzed in terms of directly measured metal:S ratios to exclude variability in cellular metal contents resulting solely from cell size (Twining *et al.*, 2004). This approach was considered superior to normalizing by P content in this study for three reasons. First, the SXRF method is more sensitive to S than to P; S has higher fluorescence yield and is less subject to interference from fluorescence from the Au grid or from Si-escape peaks in the detector caused by Ca fluorescence. Second, protein content per unit biomass is likely to be less variable than P content. Finally, changes in beamline conditions for this study made it more difficult than usual to estimate P during some of the measurement runs.

When comparing cell metal contents with zooplankton metal contents, we converted the cellular values to metal:C, as this ratio is more pertinent to mineral limitation. Carbon cannot be estimated directly using the SXRF (Twining *et al.*, 2003). Therefore, we estimated metal:C ratios by dividing the metal:S ratios by 99 (Twining *et al.*, 2004, 2011). If cellular C:S ratios vary due to varying cysteine content or changing protein:carbon ratios, this will affect our metal:carbon ratios. While cellular C can be estimated based on biovolume, we have found that such measurements agree broadly with S measurements (Twining *et al.*, 2003, 2004, 2011). Biovolume measurements are also subject to even more assumptions and potentially a range of possible errors associated with measuring cell volume on dried cells (Twining *et al.*, 2004).

RNA:DNA ratios

RNA:DNA ratios were measured on bulk size-fractionated samples because we wanted these measurements to be comparable to trace metal measurements on the same bulk fractions (Baines *et al.*, 2016). Nucleic acids of zooplankton samples were analyzed following Speekmann *et al.* (Speekmann *et al.*, 2007), with some modifications due to the large biomass in each sample. RNA and DNA of samples were extracted and stained with fluorochrome RiboGreen. Before fluorescence measurement, RNase- and DNase-free water was made by adding diethyl pyrocarbonate (DEPC) (0.1% final concentration) to distilled, deionized water. This water was incubated at room temperature for 24 h, before being autoclaved at 120°C at 15 psi for 30 min. TE (Tris−EDTA) assay buffer was made by diluting 20 × TE buffer (200 mmol L^{-1} Tris−HCl, 20 mmol L^{-1} EDTA in RNase/DNase-free water, pH 7.5, Molecular Probes) with nuclease-free water. Extraction buffer was made with 1 × TE buffer containing 0.1% Triton X-100 and 0.1 mg mL^{-1} protease (type VIII, 7−15 units mg^{-1}, Sigma) on the day of analysis. Quant-iT^{TM} RiboGreen RNA quantitation reagent (Molecular Probes®) was diluted by 200-fold with 1 × TE buffer in the dark within an hour of analysis. RNA standard (16S and 23S rRNA from *Escherichia coli*, Molecular Probes®) and DNA standard (lambda DNA, Invitrogen^{TM}) stocks were diluted with 1 × TE buffer into 4 and 2.5 μg mL^{-1}, respectively, as working standards. RNase (5.0 mg mL^{-1}) was made by dissolving RNase A (type III-A, 85−140 Kunitz unit, Sigma) in 0.01 mol L^{-1} sodium acetate (pH 5.0) and then heating to 100°C for 15 min. After cooling, bovine albumin serum (BSA) was added at 1.0 mg mL^{-1} and mixed, and pH was adjusted to 7.4 with 1 mol L^{-1} Tris−HCl solution before use.

On the day of analysis, RNA and DNA standards were diluted with 1 × TE buffer to 0−2000 and 0−1250 ng mL^{-1}, respectively. Each Eppendorf tube of zooplankton samples received 0.5 mL extraction buffer and was homogenized with an RNase/DNase/pyrogen-free plastic pellet pestle. Less than 20 μL of subsamples was transferred into a new Eppendorf tube with addition of another 0.5 mL extraction buffer and then homogenized again. Subsamples were incubated at room temperature on a TSZ scientific^{TM} orbital shaker for 1 h. After incubation, 100 μL of extracted sample or standards was added into a black Nunc^{TM} U96 MicroWell^{TM} Plate with 100 μL diluted RiboGreen reagent, and then incubated in the dark for 5 min. Fluorescence was measured by a spectrofluorometer integrated with an Infinite® F500 filter-based multimode microplate reader for RNA and DNA combined (FLC). Each well was then added with 25 μL RNase and incubated in the dark for 30 min before measuring fluorescence for DNA (FLD). RNA fluorescence was calculated as FLR = FLC − FLD. RNA and DNA concentrations were calculated from standard curves.

Data handling and statistical treatment

High Fe:S ratios and correlations between metal:S ratios and Cr:S suggest contamination in some samples (Fig. 1).

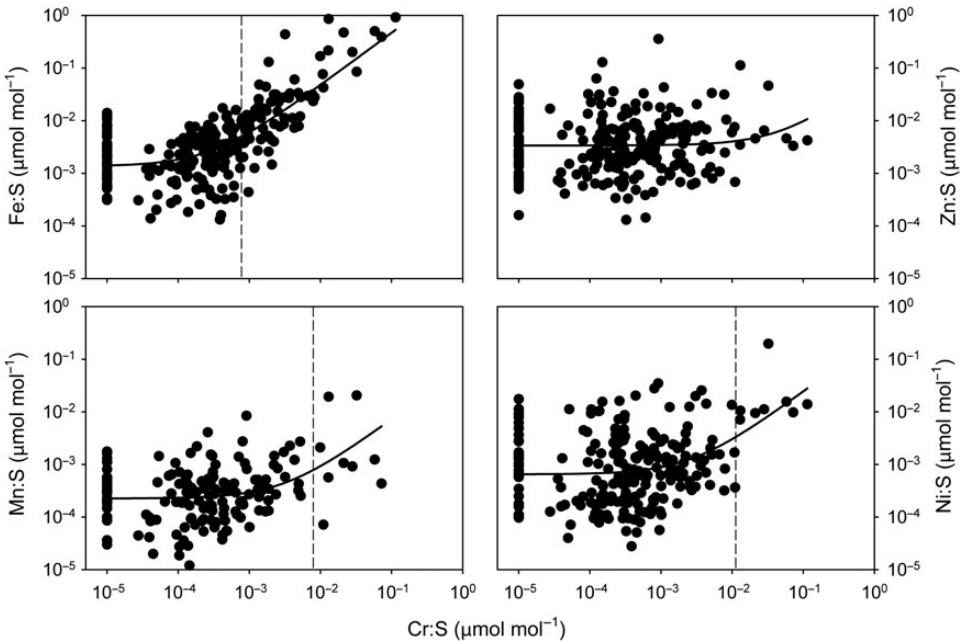

Fig. 1. Relationships of Fe:S, Zn:S, Ni:S and Mn:S with Cr:S. Each point is an observation of a single cell. The curve represents the best fit of the following model: log(Metal:S) = log[$a + b \times$ (Cr:S)]. It is used only to exemplify the relationships in each case. The vertical broken line is the cutoff value of Cr:S for each metal that renders the effect on Cr:S statistically insignificant.

This varied substantially among grids from the same sample, suggesting that handling of the grids contributed to contamination. As Fe, Cr, Mn and Ni are components of stainless steel used in the forceps that held the grids during drying, we believe this was the source. Inspection confirmed that the teflon coating on some forceps had been compromised. To remove the influence of such contamination, we first regressed the logarithm of all sulfur-specific metal concentrations against the logarithm of Cr:S. The cells for which Cr:S was not detectable were arbitrarily assigned a Cr:S value of 0.1 μmol mol^{-1} in these regressions, which was slightly less than the minimum measured value of ~0.15 μmol mol^{-1}. We sequentially removed the observations with the highest Cr:S values until the regression was no longer significant. The remaining observations were then used in subsequent statistical tests.

Outliers can have undue influence on calculated means from SXRF analyses. The cells imaged may be moribund, or the presence of inorganic particles, including metal oxides, near, on, or under cells can distort apparent cellular concentrations. Spectral interference and detector artifacts can result from excessive salt and carbonates in the sample, or from the Au in grid bars near to the cell. The proper definition of target and background regions of interest and the use of an explicit spectral model reduce, but do not eliminate, such effects. We manually excluded obvious adsorbed particles and salt crystals from further analyses. To identify and remove remaining outliers, jack-knifed studentized residuals were calculated from a two-way analysis of covariance (ANCOVA) that accounted for variation due to location, cell type and cell size (Baines *et al.*, 2011). We set the exclusion threshold so that, for a data set of n observations, there was only a 5% chance of any observation being greater than that threshold given a t-distribution. This amounts to determining the t-value at $P = 1\text{-}e^{\ln(1-0.05)/n}$. The jack-knifed studentized residual that exceeded this limit by the greatest value was removed, and the procedure was repeated until no residuals exceeded the threshold.

To assess how metal contents varied among cycles and depths sampled, diatom and flagellate Zn:S, Mn:S and Zn:S were separately analyzed by a one-way ANOVA that treated each depth and cycle combination as a distinct level. The same analysis could not be done for Fe:S of diatoms because they were too rare. To test for differences in the elemental ratios between flagellates and diatoms, we conducted a two-way ANOVA by adding cell type as a variable to the analysis described above. For each metal ratio, we also conducted a two-way ANOVA with cycle and depth as predictors. These analyses were conducted separately for diatoms and flagellates. For all tests, the influence of cell size was assessed by initially including total cellular S content as a covariate.

If zooplankton growth is limited by trace metals, there should be some correlation between RNA:DNA ratios

in mesozooplankton and the discrepancy between the metal contents of food and zooplankton tissues. Flagellates dominated autotrophic biomass in the CRD during this cruise (Taylor et al., 2016), so we first calculated the mean flagellate metal ratios for the ML and SSCM separately for each cycle. The water column average for a cycle was then taken as the average of these two values. We also determined which layer of the water column (ML or SSCM) had the lowest flagellate metal ratio, as community RNA:DNA ratios could be lower if a fraction of the community was feeding at a depth with poor quality food. Both this minimum ratio and the water-column average ratio were then divided by the corresponding metal ratios for bulk zooplankton in each of four size fractions (0.2−0.5, 0.5−1.0, 1−2 and 2−5 mm) resulting in a maximum (Max-*D*) and an average discrepancy (Avg-*D*) for each size fraction. These zooplankton metal contents are presented in a related paper (Baines *et al.*, 2016) and were determined by ICP-MS and C/N analysis of oxalate washed bulk samples collected at the same times and in the same manner as the samples used for RNA:DNA analysis to ensure comparability. These two discrepancy indices were then used in regressions predicting RNA:DNA ratio for each size class and cycle ($n = 16$). To account for the influence of food availability, we also included the mean autotrophic nanoplankton biomass as a possible predictor (as reported in Taylor *et al.*, 2016).

All continuous variables were log-transformed prior to analysis to meet the assumptions of the statistical tests, including normally distributed residuals and constant variance. Cells that could not be unambiguously assigned to a cell type were not used in these analyses. Critical *P*-values were set to 0.05 for statistical tests, but we report *P*-values when possible. *Post hoc* tests of differences between group means are based on Tukey's honest significant difference test (Tukey's HSD, Tukey, 1949). All statistical analyses were performed in JMP 7.02 (SAS Institute, Cary, NC, USA).

RESULTS

A total of 233 cells were analyzed for elemental content via SXRF, including 153 flagellates and 45 diatoms. The Cr:S thresholds above which observations were excluded from further analyses were 0.78 mmol mol^{-1} for Fe:S, 7.95 mmol mol^{-1} for Mn:S and 11.2 mmol mol^{-1} for Ni:S. Zn:S was not related to Cr:S. These thresholds resulted in exclusion of 64, 11 and 8 cells, respectively, for Fe:S, Mn:S and Ni:S (Table I). The geometric means and standard errors of the ratios varied among the elements with Zn:S = 9.6 ± 1.9 mmol mol^{-1}, Fe:S = 3.3 ± 0.25 mmol mol^{-1}, Ni:S = 2.25 ± 0.31 mmol mol^{-1} and Mn:S = 0.47 ± 0.05 mmol mol^{-1} (Table II)

Diatoms had a 3-fold higher Fe:S than flagellates ($P < 0.0001$, *F*-test; Fig. 2) after accounting for differences among sites and depths. No other metal ratio differed significantly among cell types, although the higher Ni:S content of diatoms was borderline significant ($P = 0.08$, *F*-test).

Cellular metal contents varied substantially between depths (Fig. 3). The ratio of Ni:S was 8-fold higher for diatoms in the ML than in the SSCM ($P = 0.0028$). For flagellates, the difference was 6-fold ($P < 0.0001$). The ratio of Zn:S in diatoms was 2.4-fold higher in the ML than in the SSCM ($P = 0.011$). The Zn:S of flagellates was 20% higher in ML waters, but the difference was not significant. The ratio of Fe:S showed the opposite pattern to that of Zn:S, being almost 2-fold higher in flagellates from the SSCM than in the same cell type from the ML ($P = 0.001$). Although diatoms exhibited 60% higher Fe:S in the SSCM than in the ML, the difference was not significant ($P = 0.25$).

The mean metal ratios varied substantially among stations, with different patterns among cell types (Fig. 4). For flagellates, Fe:S values during Cycles 2 and 3 were about half those during Cycles 1 and 4 ($P = 0.017$), while Cycle 5 was intermediate. Zn:S in flagellates varied among cycles ($P < 0.0001$), but Cycle 1 had by far the highest

Table I: Numbers of cells analyzed by each cell types and for each cycle and depth

Cycle	Lat. (°N)	Long. (°N)	Layer	Depth (m)	Diatoms	Flagellates	Picoautotrophs
1	9.715	87.004	ML	15	6 (6)	10 (7)	15 (8)
			SSCM	27.5	0 (0)	18 (15)	16 (14)
2	9.037	90.564	ML	10–15	5 (1)	9 (4)	3 (1)
			SSCM	22–24	8 (0)	18 (14)	0 (0)
3	10.416	92.916	ML	10–12	3 (3)	28 (25)	1 (1)
			SSCM	24	3 (2)	17 (16)	0 (0)
4	8.546	90.399	ML	10	11 (5)	14 (8)	0 (0)
			SSCM	30	2 (2)	25 (18)	0 (0)
5	8.877	88.465	ML	15	7 (6)	14 (13)	0 (0)

Numbers in parentheses are those remaining after removing samples with high Cr:S. Depth ranges represent different sample collection casts.
ML, mixed layer; SSCM, subsurface chlorophyll maximum.

Table II: Summary of average ratios of Fe, Mn, Ni and Zn to S (μmol mol^{-1}) for different cycles, depths and cell types

		Fe:S				Mn:S				Ni:S				Zn:S			
		ML		SSCM		ML		SSCM		ML		SSCM		ML		SSCM	
C	Cell	Avg	SE	Avg	SE	Avg	SE	Avg	SE	Avg	SE	Avg	SE	Avg	SE	Avg	SE
1	F	3.79	0.87	3.03	0.55	0.41	0.15	0.36	0.12	0.80	0.22	1.31	0.95	4.13	0.84	25.0	8.67
2	F	2.50	0.35	2.18	0.73	0.38	0.12	0.2	0.04	5.22	2.03	0.81	0.12	2.93	0.57	0.92	0.1
3	F	1.02	0.19	2.50	0.34	0.42	0.08	0.75	0.2	4.78	0.91	0.14	0.02	11.7	2.24	2.58	0.5
4	F	1.17	0.25	4.88	1.11	0.34	0.11	0.16	0.04	2.07	0.5	0.79	0.25	5.14	1.52	11.0	3.63
5	F	1.97	0.66	nd	nd	0.17	0.12	nd	nd	0.13	0.03	nd	nd	2.94	0.58		
1	D					0.28	0.16	nd	nd	1.95	0.53	nd	nd	10.1	3.62	nd	nd
2	D					0.41	0.11	0.26	0.06	5.51	4.04	0.58	0.15	4.64	1.07	1.09	0.27
3	D					2.58	1.81	0.82	0.23	10.3	2.47	0.47	0.22	4.30	0.77	4.43	2.49
4	D					0.15	0.02	0.32	0.1	1.73	0.29	0.71	na	2.85	0.67	1.62	0.84
5	D					0.74	0.64	nd	nd	0.62	0.09	nd	nd	6.95	2.42	nd	nd

ML, mixed Layer; SSCM, subsurface chlorophyll maximum; C, cycle; D, diatom; F, flagellate; SE, standard error.

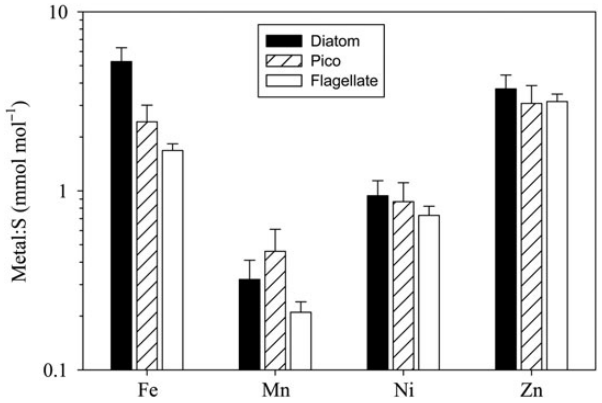

Fig. 2. Geometric mean values ± SE for Fe:S, Zn:S, Mn:S and Ni:S. Means are corrected for effects of Cycle and depth via an ANOVA. Dark bars, diatoms; hatched bars, picocyanobacteria; open bars, flagellates. Error bars, SE.

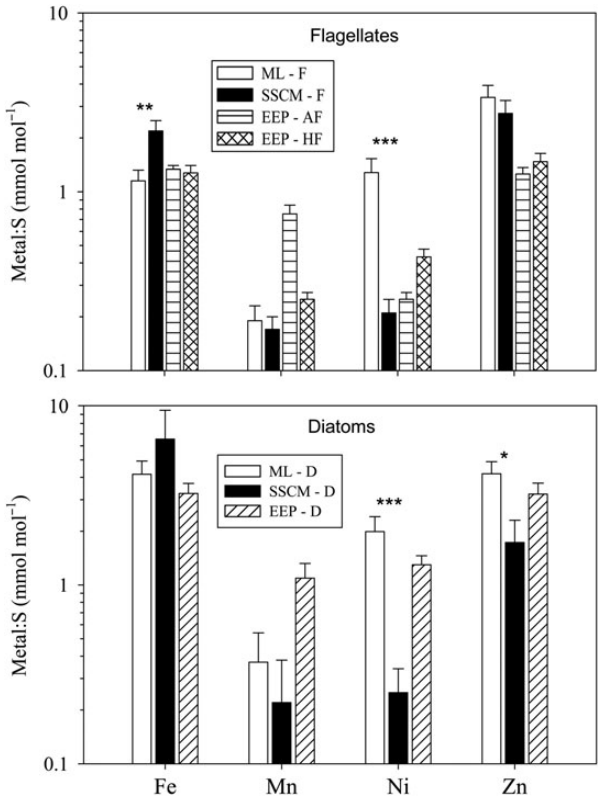

Fig. 3. Effects of depth on Fe:S, Zn:S, Mn:S and Ni:S for flagellates (top panel) and diatoms (bottom panel) from both the CRD (this study) and the EEP (Twining *et al.*, 2011). Open bar, surface mixed layer (ML); closed bar, subsurface chlorophyll *a* maximum (SSCM); horizontal striped, autotrophic flagellates from the EEP; cross hatched, heterotrophic flagellates from the EEP; diagonal hatched, diatoms from EEP. Statistical tests: *$0.05 < P < 0.01$, **$0.01 < P < 0.001$, ***$0.001 < P < 0.0001$. Error bars, SE.

ratio, 6.4-fold greater than Cycle 2, 4.3-fold greater than Cycle 5 and 2.2-fold greater than Cycles 3 and 4. Diatoms did not show significant variation in Fe:S among cycles ($P = 0.12$), although error bars were large due to the small number of cells included in the analysis. Diatoms exhibited some variation in Zn:S among cycles, with the lowest values for Cycles 2 and 4, but the differences were only borderline significant ($P = 0.07$).

The mean flagellate Fe:C was uniformly lower than measured in mesozooplankton biomass (Fig. 4). For Cycles 2 and 3, Fe:C ratios in flagellates were almost 3× lower than in the 2–5 mm mesozooplankton fraction, which had the lowest Fe:C in tissues, and >5-fold lower than the 0.2–0.5 mm fraction, which had the highest tissue Fe:C. Diatoms, by comparison, exhibited Fe:C ratios in the same range as the tissue Fe:C ratios of the different zooplankton fractions. The Zn:C ratios for both diatoms and flagellates were generally similar to or larger than the ratios measured for the two smallest mesozooplankton size classes. The exceptions included Cycle 2, for which Zn:C for largest

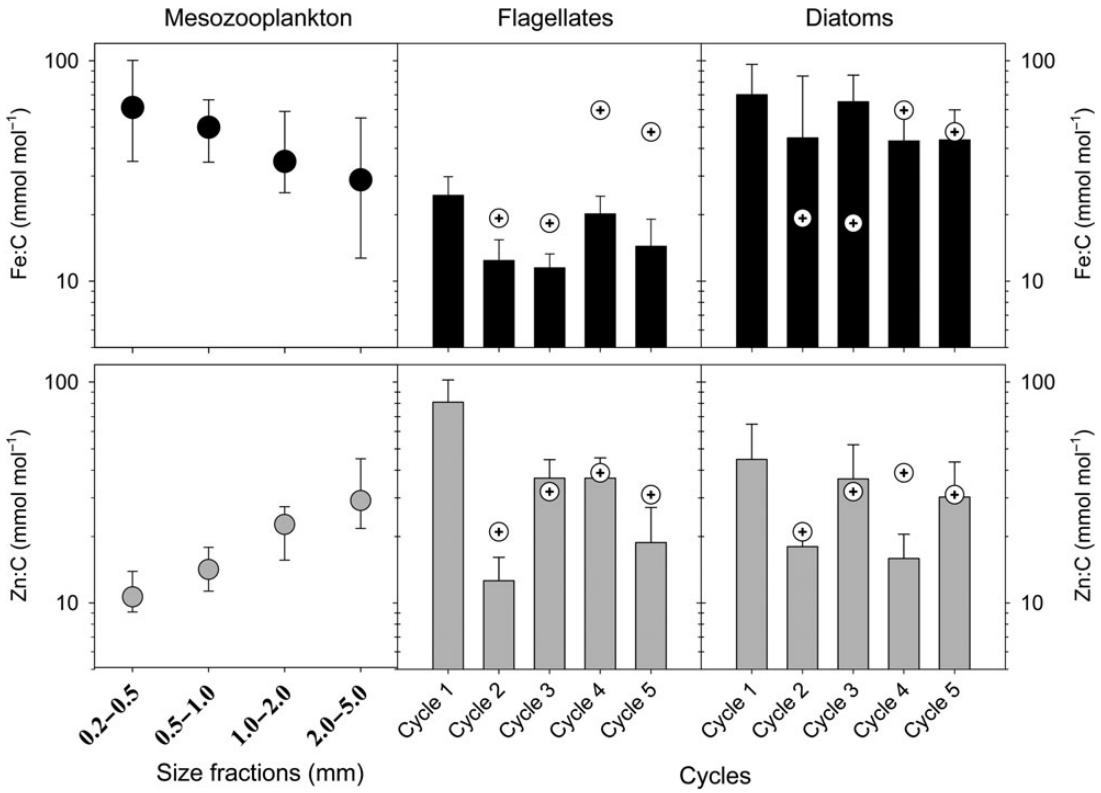

Fig. 4. Comparison of metal ratios in mesozooplankton and in single cells. (Left panels) Scatter plots of mesozooplankton Fe:C and Zn:C for different size classes as reported in Baines *et al.* (2016). (Middle panels) Geometric means of Fe:C and Zn:C for all flagellated cells in the water column for each cycle (bars). (Right panels) Geometric means of Fe:C and Zn:C for diatoms in the water column for each cycle (bars). Metal ratios for the largest zooplankton size fraction are included for reference in both the middle and left panels (open circles with cross-hairs). Error bars, SE. Grey bars and symbols refer to Zn:C, while black bars and samples refer to Fe:C.

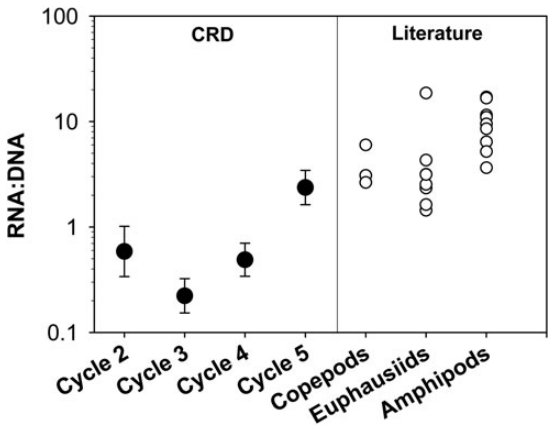

Fig. 5. On the left panel are mean RNA:DNA ratios for mesozooplankton for Cycles 2–5. On the right-hand side, the open circles are literature estimates.

zooplankton size class (2–5 mm) was almost 2.4-fold higher than the Zn:S in flagellated protists and 1.6-fold higher than in diatoms, and Cycle 4, for which the Zn:C of the same size class was 1.8-fold larger than diatoms.

Average RNA:DNA ratios of mixed zooplankton for the cycles ranged between 0.44 and 2.6 (Fig. 5). The highest ratio was for Cycle 5, located at the eastern edge of the CRD. The ratios for Cycles 2–4 were all low relative to published study averages, while the value for Cycle 5 was within the lower half of the published range (Fig. 5, Table III). No measurements of RNA:DNA were made for Cycle 1, which was clearly outside the CRD. RNA:DNA ratios from all cycles, including those from outside the dome area, did not show any diel pattern nor any variation among size fractions ($P = 0.56$). RNA:DNA ratios were not significantly related to any measure of the discrepancy (D) between Fe:C and Zn:C ratios in zooplankton and flagellate cells (Table IV). However, RNA:DNA was significantly related to biomass of autotrophic nanoplankton ($P = 0.004$; Table IV). The maximum discrepancy between Zn:C in flagellates and zooplankton tissues (max-$D_{Zn:C}$) was borderline significant ($P = 0.06$) as a predictor of RNA:DNA when included in a bivariate regression, with biomass of autotrophic nanoplankton the other predictor (Fig. 6, Table IV).

Table III: RNA:DNA ratios in zooplankton from this and other studies

Taxon	Species	Region	RNA:DNA	Reference
Copepods	Cyclopoid	CRD	2.5 ± 0.41	This study
	Calanoid	CRD	1.4 ± 0.29	This study
Copepods	*Acartia bifilosa*	Eastern Gotland basin	1.9–5	Gorokhova (2003)
	Calanus finmarchicus	Raunefjord, Bergen	4–9	Hansen *et al.* (2003)
	Mixed calanoids	N Pacific, Bering Sea	1.5–4.7	Ikeda *et al.* (2007)
Euphausiids	*Cyllopus lucasii*	Weddell Sea	4.3 ± 1.6	Donnelly *et al.* (2004)
	Vibilia stebbingi	Same as above	18.4 ± 9.2	Same as above
	Galiteuthis glacialis	Same as above	2.5 ± 0.33	Same as above
	Euphausia triacantha	Same as above	1.4 ± 0.30	Same as above
	Euphausia superba	Same as above	1.9–2.9	Same as above
	Thysanoessa macrura	Same as above	2.2–4.6	Same as above
	Cyphocaris faueri	Same as above	2.5	Same as above
	Cyphocaris richardi	Same as above	2.1–4.7	Same as above
	Cleonardo longipes	Same as above	1.6	Same as above
Amphipods	*Parandania boecki*	Same as above	6.4	Same as above
	Cyllopus lucasii	Same as above	3.4–3.9	Same as above
	Hyperiella antarctica	Same as above	11.5	Same as above
	Hyperoche medusarum	Same as above	11.0	Same as above
	Megalanceola remipes	Same as above	9.5	Same as above
	Megalanceola stephenseni	Same as above	8.6	Same as above
	Primno macropa	Same as above	11.4–25.5	Same as above
	Themisto gaudichaudi	Same as above	5.2	Same as above
	Vibilia stebbingi	Same as above	15.1–18.4	Same as above
Decapods	*Gennadas kempi*	Same as above	1.1 ± 0.09	Same as above
	Nematocarcinus lanceopes	Same as above	2.1 ± 0.38	Same as above
	Pasiphaea scotiae	Same as above	2.8–4.9	Same as above
	Petalidium foliaceum	Same as above	0.66	Same as above
Isopods	*Anuropus australis*	Same as above	0.59	Same as above
Mysids	*Boreomysis rostrata*	Same as above	1.1	Same as above
	Gnathophausia gigas	Same as above	0.36	Same as above
Ostracods	*Gigantocypris mulleri*	Same as above	1.3–1.9	Same as above

Table IV: Summary of statistics related to regressions predicting RNA:DNA ratios in mesozooplankton

	Univariate models		Bivariate models	
Predictors	*F*-value	*P*-value	*F*-value	*P*-value
ANBM	11.9	0.0039	17.6	0.001
Avg-$D_{Zn:C}$	0.005	0.94	1.89	0.19
Avg-$D_{Fe:C}$	3.35	0.089	0	0.99
Max-$D_{Zn:C}$	0.528	0.48	4.21	0.061
Max-$D_{Fe:C}$	0.013	0.91	0.046	0.83

ANBM, autotrophic nanoplankton biomass; Avg-*D* and Max *D* are the average and maximum discrepancies between the metal ratios of flagellated cells and co-occurring mesozooplankton. The subscripts indicate the metal ratio being compared. Bivariate models all include ANBM as a predictor. Values with $P<0.1$ are in bold.

DISCUSSION

The present study is one of the first to make a direct comparison between trace element composition of mesozooplankton and their food. In some respects, conditions in the CRD during this cruise were not ideal for producing trace metal limitation of primary production (Landry *et al.*, 2016a). Moderate El Niño conditions prior to the cruise led to cloudy skies, warm surface waters that limited upwelling and anomalously low autotrophic biomass, as seen in suppressed surface concentration of Chl *a* in satellite images relative to other summers. With reduced or only sporadic supply of deep water deficient in trace metals, conditions were not ideal for identifying signatures of trace metal limitation, so the analyses presented here represent a rather strict test. Below, we discuss some of the patterns in cell elemental content and the potential for these ratios to lead to mineral limitation of mesozooplankton, or to allow mesozooplankton to escape limitation through selective use of rich resources.

Evidence for Fe and Zn limitation of protists

Differences between the cellular Fe ratios of diatoms and other cells (Fig. 2) corresponded well with previous measurements from the EEP (Twining *et al.*, 2011), another HNLC region where the phytoplankton community has been shown to be Fe-limited (Coale *et al.*, 1996; Brzezinski *et al.*, 2011). The Fe ratios of diatoms from the EEP and the CRD are similar to those of phytoplankton from regions of the Atlantic not thought to be Fe-limited (Twining and Baines, 2013). The dominant diatoms in

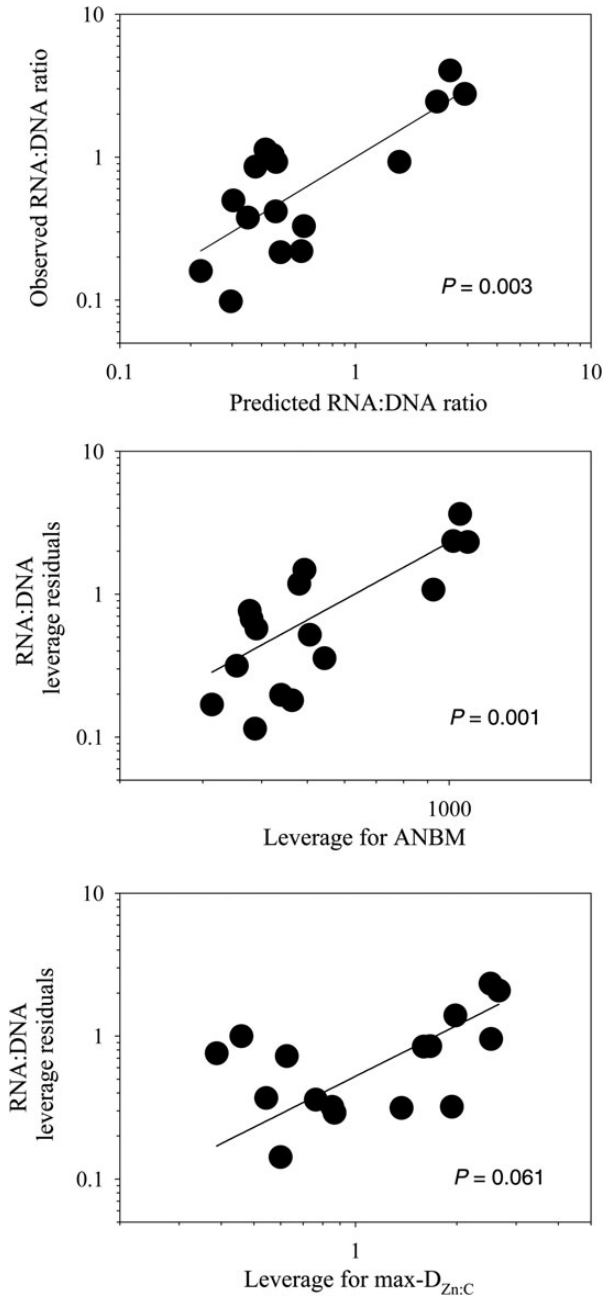

Fig. 6. Plots relating to bivariate regression of RNA:DNA ratios on autotrophic nanoplankton biomass (ANBM) and the maximum discrepancy between Zn:C ratios of flagellate cells and mesozooplankton (max-$D_{Zn:C}$). (Upper panel) Predicted versus observed values for the mode. *P*-value designates significance of whole model. (Middle panel) Leverage of RNA:DNA residuals plotted against leverage of ANBM. (Bottom panel) Leverage of RNA:DNA residuals plotted against residuals of max-$D_{Zn:C}$. *P*-values in the lower two panels relate to significance of each predictor variable.

the EEP were small (<20 μm) thin pennates belonging to the genus *Pseudo-nitszchia*, which has been shown to store Fe within the protein ferritin (Marchetti *et al.*, 2009). Indeed, small pennates in the EEP exhibited substantial luxury uptake of Fe when it was added to experimental mesocosms (Brzezinski *et al.*, 2011). We postulated at the time that these cells may sequester Fe released from ligands by photochemical reduction in Fe during intense daytime insolation at the equator (Twining *et al.*, 2011). The cells that formed the bulk of the diatoms imaged from the CRD were very similar in appearance to the cells imaged in that prior study of the EEP and had similar cellular Fe ratios (Fig. 3).

In contrast, non-diatoms in the CRD exhibited Fe ratios suggestive of Fe-limitation. During Cycles 2 and 3 in the CRD, the average flagellate Fe ratios for the water column approached those seen in the Fe-limited EEP. In fact, the average cellular Fe ratios for flagellates in the ML across the entire CRD were very similar to those observed in the ML in the Fe deplete EEP (Fig. 3) and 2-fold lower than observed in Fe replete regions in the north Atlantic (Twining and Baines, 2013). Moreover, the Fe ratios of flagellates during these two cycles were 2-fold lower than during Cycle 1 (Fig. 4), which was in a more coastal location outside the CRD that appeared to be Fe-replete (Selph *et al.*, 2016). Interestingly, flagellate Fe ratios were also relatively high during Cycle 4, which occurred at a location very near to Cycle 2 in the central area of the CRD (Fig. 4). This may reflect an increase in upwelling at this site just prior to sampling (Landry *et al.*, 2016a; Selph *et al.*, 2016). The low cellular Fe ratios at some stations, especially within the ML (Table II, Fig. 3), suggest that Fe is a factor shaping community composition and production of autotrophs in the CRD. More extreme Fe limitation might have been observed had the CRD not been experiencing mild El Niño conditions. Instead, the increased stratification and cloudiness limited upwelling of relatively Fe-deplete waters and retarded the ability of autotrophs to grow and exhaust resources.

Depletion of Zn relative to phosphorus in surface waters suggests that Zn may also be an important limiting factor for phytoplankton (Chappell *et al.*, 2016). However, we saw only variable evidence for Zn stress in cell elemental composition, perhaps reflecting the borderline development of typical HNLC conditions in the CRD or the region's spatial complexity (Table II, Fig. 4). While cellular Zn ratios in the CRD were much lower than in high Zn regions of the Southern Ocean (Twining *et al.*, 2004), the Zn ratios in CRD diatoms were actually quite similar to those found previously for diatoms in the EEP (Twining *et al.*, 2011), where Fe is typically considered the most limiting nutrient (Coale *et al.*, 1996; Brzezinski *et al.*, 2011). The 2- to 3-fold higher cellular Zn ratios for flagellates in the CRD compared with the EEP also argue against Zn limitation for the region as a whole (Fig. 3). There was substantial variability in cellular Zn ratios

among the cycles (Fig. 4). Flagellates during Cycle 1 in particular had quite high cellular Zn ratios, as might be expected given the strong coastal influence on that set of measurements.

In summary, patterns in cellular Fe and Zn among cell types within the CRD very much resemble the EEP. This suggests that patterns described here for the CRD may have relevance to other Fe-limited areas of the tropics.

Patterns in cellular Fe and Zn

This is one of the first studies to assess depth differences in trace elemental contents of single cells. Several patterns emerge from the data that might relate to spatial variability in the quality of food resources for mesozooplankton. First, the two potentially limiting elements, Fe and Zn, displayed opposite trends with depth (Fig. 3). Cellular Fe ratios were lower in the ML than in the SSCM, as might be expected if there is an increased cellular Fe requirement under lower light (Raven *et al.*, 1999) or because the main source of dissolved Fe is from deeper in the water column. Slower growth under poorer light conditions at depth can also cause this pattern (Sunda and Huntsman, 1997; Finkel *et al.*, 2006). In any case, the results suggest that cells from the SSCM should be high quality food for mesozooplankton.

In contrast, cellular Zn ratios in diatoms and flagellates were generally higher in the ML than in the SSCM (Fig. 3). Such a pattern does not seem consistent with the idea of a limiting nutrient diffusing upward from depth. As there is no other direct source of Zn to surface waters, the high cellular Zn ratios in the ML probably reflect a biochemical response to chemical and/or physical challenges unique to these depths. Zinc is a component of many enzymes that perform a range of functions. The >0.2 μmol L^{-1} phosphate in the CRD (Chappell et al., 2016; Selph *et al.*, 2016) should make substantial allocation of Zn to alkaline phosphatase unnecessary. The higher cellular Zn ratios could also reflect an investment by eukaryotic phototrophs in Cu−Zn superoxide dismutases (CuZnSOD) which are found in dinoflagellates and in plastids generally (Wolfe-Simon *et al.*, 2005). Such an investment may be favored in variable light environments like those during this cruise, as cells may tune their photosynthetic machinery to lower light intensities during cloudy periods but periodically experience full tropical sun that can result in the production of dangerous reactive oxygen species. Finally, high Zn quotas could reflect substantial investments in Zn-containing carbonic anhydrase in carbon concentrating mechanisms that might be favored in the warm surface waters of the CRD where demand for CO_2 is high, but CO_2 is scarce (Morel *et al.*, 1994).

Mn:S and Ni:S as possible tracers

We included measurements of Mn and Ni in this study because these two elements were correlated with Fe and Zn contents of zooplankton food, and therefore may constitute tracers for sources of dietary metals if they exhibit unique spatial or taxonomic signatures. Cellular Mn ratios were quite similar to previous measurements from the EEP and elsewhere, except that diatoms were not significantly enriched in Mn (Fig. 2). Depth also had no significant influence on cellular Mn ratios (Fig. 3). As a consequence, Mn does not appear to be a useful tracer for Fe or Zn sources. Ni may be more useful as a tracer due to its unusual distribution. Perhaps the most striking pattern that we found was that cellular Ni-ratios for both diatoms and flagellates were 8- to 10-fold higher in the ML than in the SSCM (Fig. 3). This pattern mirrors the 80% greater Ni content of *Synechococcus* cells at the surface in the Sargasso Sea compared with cells collected from the SSCM (Twining *et al.*, 2010). The observed Ni concentrations in surface waters are the highest yet observed for this element. Nickel is used as a cofactor in urease, which is typically used to assimilate nitrogen (Oliveira and Antia, 1986; Price and Morel, 1991). Expression of urease may be induced when nitrate is rare or inaccessible due to reduced nitrogen reductase activity due to Fe-limitation. However, nitrate remained at near micromolar concentrations in surface waters in the CRD (Chappell et al., 2016; Selph *et al.*, 2016). Urease is also an alternative way to acquire nitrogen when Fe is so rare that cells cannot make Fe-rich nitrogen reductase needed to assimilate nitrate into amino acids (Price and Morel, 1991). As such, this pattern may be another indirect indication that Fe availability constrains the capacities of autotrophs within surface layers of the CRD. Alternatively, high cellular Ni content could also reflect the production of Ni-SODs in response to oxidative stress in surface waters (Twining *et al.*, 2012). While Ni-SODs are typically thought of as prokaryotic, they have been observed in genomes of many eukaryotic phytoplankton, possibly reflecting lateral transfer (Cuvelier *et al.*, 2010).

Potential for mineral limitation of mesozooplankton production

This study is one of the first attempts to compare directly the elemental compositions of co-occurring mesozooplankton and single-celled algae. That said, estimating the potential for mineral limitation of zooplankton production via a simple comparison between trace metal composition of mesozooplankton and single-celled plankton requires some caveats.

First, the Fe:C ratio in zooplankton tissues is not necessarily the same as the critical Fe:C in prey below which mineral limitation of zooplankton production occurs. One has to account for the relative ability of zooplankton to assimilate both Fe and C from food, and to retain these two elements once assimilated. However, calculations of this minimum limiting Fe:C threshold in food for the coastal copepod *A. tonsa* show that it is always the same or greater than the Fe:C of zooplankton tissues (Chen *et al.*, 2014). While carbon lost through respiration tends to reduce the limiting threshold Fe:C in food relative to tissue Fe:C, this effect is counteracted by the relatively poor assimilation of Fe from food relative to C and specific Fe excretion rates of ~20% day^{-1} (Schmidt *et al.*, 1999; Chen *et al.*, 2014). As of yet, there has been no indication that copepods can adjust either their assimilation or their respiration to Fe content of their food enough to adjust their limiting threshold to match their environment (Chen *et al.*, 2014). Furthermore, it is important to note that such adjustments, where they to occur, would not come without costs to zooplankton grazers. Increasing respiration rates necessarily means a reduction in carbon allocated to growth, and therefore implies lower growth efficiency and growth rate. Until better information exists on the handling of trace elements at low concentrations by zooplankton *in situ*, we can only assume that the elemental content of zooplankton is a minimum estimate of the critical limiting threshold Fe:C.

On that basis, the smallest zooplankton size fraction, which has the higher tissue Fe:C ratios, likely experiences quite severe Fe limitation (Fig. 4). However, it is also not certain that Fe:C content of the smallest fraction is representative of a real requirement. The decline in Fe:C with increasing mesozooplankton size was correlated to a decline in Al and Ti content, which suggests that a strong lithogenic signal affected the smaller size fractions the most (Baines *et al.*, 2016). The use of typical Fe:Al ratios in clays to correct zooplankton Fe had little effect, suggesting the "lithogenic signal" was indirect in nature and not due to direct contributions of clay particles to the mesozooplankton samples (Baines *et al.*, 2016). Just to be cautious, we used only samples that were low in Al and Ti to determine a lower bound for mesozooplankton Fe:C of ~20 μmol mol^{-1} for the nighttime migrant community, and ~30 μmol mol^{-1} for the resident surface community (Baines *et al.*, 2016). Only Cycles 1 and 4 exhibited flagellate Fe:C ratios approaching these values (Fig. 4). For the other cycles, the Fe:S for flagellates was 50–100% lower than for mesozooplankton.

The use of diatoms as an iron-rich dietary supplement could redress the apparent shortfall in Fe, but that requires diatoms to be abundant enough to constitute a substantial portion of the diet. In the CRD, diatoms never accounted for more than 2% of autotrophic biomass during this cruise (Taylor *et al.*, 2016); however, diatoms accounted for ~10% of the diet of mesozooplankton (Landry *et al.*, 2016). Phytoplankton community structure may therefore play a key role in determining whether mesozooplankton can avoid mineral limitation by Fe.

The case for Zn limitation of zooplankton growth is more complex. Zinc is assimilated more efficiently than Fe by copepods (Reinfelder and Fisher, 1991). As a consequence, mesozooplankton Zn:C may not be as conservative an estimate of the critical threshold metal ratio in food as is the mesozooplankton Fe:C. On the other hand, the Zn:C ratios in mesozooplankton are not affected by lithogenic metal and therefore indicate the actual metal content of tissues. Still, only for the largest size fraction of mesozooplankton in Cycles 1 and 2 was the Zn:C content of the flagellate community lower (Fig. 4). We were able to show a correlation between RNA:DNA ratios measured on zooplankton size fractions and two variables: the nanoautotrophic biomass and the maximum difference between zooplankton and flagellate Zn:C (Fig. 6, Table IV). The fact that flagellate Zn:C predicts zooplankton RNA:DNA even though it is comparable to mesozooplankton Zn:C suggests that the later may be a conservative estimate of the Zn:C threshold for mineral limitation.

Finally, two lines of evidence suggest that mesozooplankton production was depressed in the CRD. The RNA:DNA ratios measured in this study are generally on the low side of what have been measured for samples collected from other open-ocean areas, e.g. 0.3–4.7 in mixed copepods in the North Pacific (Ikeda *et al.*, 2007), and 1.7–18.4 in euphausiids in the Weddell Sea (Donnelly *et al.*, 2004). If low RNA:DNA ratios reflect low growth rate, we expect mesozooplankton in the CRD to also show low P content and low P:C due to lower production of rRNA (Sterner and Elser, 2002). This low P content is in fact observed (Baines *et al.*, 2016). It is unlikely that P-limitation causes such low P-content because phosphate was >0.2 μmol L^{-1} in surface waters within the CRD (Chappell et al., 2016; Selph *et al.*, 2016).

DNA contents vary widely among species (Hessen and Persson, 2009), so bulk RNA:DNA ratios may not only reflect growth rates, but also differences in species composition. The bulk values should be a summation of the species values for a community, so our results still indicate that the species-specific RNA:DNA in the CRD was low compared with species-specific literature values. However, most of the literature values come from high latitudes. The difference in RNA:DNA may not reflect differences in growth rate if CRD species possessed systematically higher DNA contents than typical of communities elsewhere. Counter to this possibility, it is usually the high-latitude

crustacean plankton that have systematically higher DNA contents, which should reduce RNA:DNA ratios (Hessen and Persson, 2009). Also, the range of RNA:DNA measured in samples ranged from 0.2 to 23.4, which includes nearly the full range of literature values (Table III). With respect to the regression results, the added random variation due to changing species composition should have made it harder to detect relationships between bulk RNA:DNA ratios and autotrophic biomass or prey trace metal contents. While it is encouraging that sensible patterns emerged from those analyses, some caution is nonetheless suggested in interpreting those patterns.

CONCLUSIONS

We have presented evidence that trace metal concentrations may be low enough in the CRD to influence the composition of single-celled plankton and their quality as food for zooplankton. There is also evidence that zooplankton growth and reproduction is limited in the CRD. Insofar as diatoms are Fe rich in the CRD, the relative abundance of diatoms could be an important factor determining the likelihood of mineral limitation of zooplankton biomass by trace metals. Selective predation on diatoms should be favored if diatoms are abundant enough to support the zooplankton population. To really assess whether mineral limitation of zooplankton by trace metals is possible, more needs to be known about the carbon and trace metal economies of zooplankton in chronically Fe-limited regions.

DATA ARCHIVING

The cellular elemental contents, zooplankton elemental composition and RNA:DNA ratios are archived at the Biological and Chemical Oceanography Data Management Office at http://www.bco-dmo.org/project/537956. Other hydrological, chemical and biological observations are accessible at http://www.bco-dmo.org/project/515387.

ACKNOWLEDGEMENTS

Thanks to crew of R/V Melville and the cruise participants, especially to J. Moffett for the use of TM-clean rosette, and P.D. Chappell for help collecting TM-clean samples. The use of the Advanced Photon Source, an Office of Science User Facility operated for the US Department of Energy (DOE) Office of Science by Argonne National Laboratory, was supported by the US DOE under contract number DE-AC02-06CH11357.

FUNDING

US National Science Foundation grants OCE-0962201 and OCE-1131139 to S.B.B. and OCE-0826626 to M.R.L.

REFERENCES

Ahlgren, N. A., Noble, A., Patton, A. P., Roache-Johnson, K., Jackson, L., Robinson, D., Mckay, C., Moore, L. R. *et al.* (2014) The unique trace metal and mixed layer conditions of the Costa Rica upwelling dome support a distinct and dense community of *Synechococcus*. *Limnol. Oceanogr.*, **59**, 2166–2184.

Anderson, T. R. and Hessen, D. O. (1995) Carbon or nitrogen limitation in marine copepods. *J. Plankton Res.*, **17**, 317–331.

Aumont, O., Maier-Reimer, E., Blain, S. and Monfray, P. (2003) An ecosystem model of the global ocean including Fe, Si, P colimitations. *Global Biogeochem. Cycles*, **17**, GB1745.

Baines, S. B., Chen, X., Twining, B. S., Fisher, N. S. and Landry, M. R. (2016) Factors affecting Fe and Zn contents of mesozooplankton from the Costa Rica Dome. *J. Plankton Res.*, **38**, 331–347.

Baines, S. B., Twining, B. S., Vogt, S., Balch, W. M., Fisher, N. S. and Nelson, D. M. (2011) Elemental composition of equatorial Pacific diatoms exposed to additions of silicic acid and iron. *Deep-Sea Res. II*, **58**, 512–523.

Bottrell, H. H., Duncan, A., Gliwicz, Z. M., Grygierek, E., Herzig, A., Hillbrichtilkowska, A., Kurasawa, H., Larsson, P. *et al.* (1976) Review of some problems in zooplankton production studies. *Norw. J. Zool.*, **24**, 419–456.

Broenkow, W. W. (1965) The distribution of nutrients in the Costa Rica Dome in the eastern tropical Pacific ocean. *Limnol. Oceanogr.*, **10**, 40–52.

Brzezinski, M. A., Baines, S. B., Balch, W. M., Beuchere, C., Chai, F., Dugdale, D. G., Krause, J. W., Landry, M. R. *et al.* (2011) Co-limitation of diatoms by iron and silicic acid in the equatorial Pacific. *Deep-Sea Res. II*, **58**, 493–511.

Chappell, P. D., Vedmati, J., Selph, K. A., Cyr, H. A., Jenkins, B. D., Landry, M. R. and Moffett, J. W. (2016) Preferential depletion of zinc within Costa Rica Upwelling Dome creates conditions for zinc co-limitation of primary production. *J. Plankton Res.*, **38**, 244–255.

Chen, X., Baines, S. B. and Fisher, N. S. (2011) Can copepods be limited by the iron content of their food? *Limnol. Oceanogr.*, **56**, 451–460.

Chen, X., Fisher, N. S. and Baines, S. B. (2014) Influence of algal iron content on the assimilation and fate of iron and carbon in a marine copepod. *Limnol. Oceanogr.*, **59**, 129–140.

Coale, K. H., Johnson, K. S., Fitzwater, S. E., Gordon, R. M., Tanner, S., Chavez, F. P., Ferioli, L., Sakamoto, C. *et al.* (1996) A massive phytoplankton bloom induced by an ecosystem-scale iron fertilization experiment in the equatorial Pacific Ocean. *Nature*, **383**, 495–501.

Cuvelier, M. L., Allen, A. E., Monier, A., Mccrow, J. P., Messié, M., Tringe, S. G., Woyke, T., Welsh, R. M. *et al.* (2010) Targeted metagenomics and ecology of globally important uncultured eukaryotic phytoplankton. *Proc. Natl Acad. Sci. USA*, **107**, 14679–14684.

Donnelly, J., Kawall, H., Geiger, S. P. and Torres, J. J. (2004) Metabolism of Antarctic micronektonic crustacea across a summer ice-edge bloom: respiration, composition, and enzymatic activity. *Deep-Sea Res. II*, **51**, 2225–2245.

Elser, J. J. and Hassett, R. P. (1994) A stoichiometric analysis of the zooplankton–phytoplankton interaction in marine and fresh-water ecosystems. *Nature*, **370**, 211–213.

Elser, J. J. and Urabe, J. (1999) The stoichiometry of consumer-driven nutrient recycling: theory, observations, and consequences. *Ecology*, **80**, 735–751.

Fiedler, P. C. (2002) The annual cycle and biological effects of the Costa Rica Dome. *Deep-Sea Res. I*, **49**, 321–338.

Finkel, Z. V., Quigg, A., Raven, J. A., Reinfelder, J. R., Schofield, O. E. and Falkowski, P. G. (2006) Irradiance and the elemental stoichiometry of marine phytoplankton. *Limnol. Oceanogr.*, **51**, 2690–2701.

Franck, V. M., Bruland, K. W., Hutchins, D. A. and Brzezinski, M. A. (2003) Iron and zinc effects on silicic acid and nitrate uptake kinetics in three high-nutrient, low-chlorophyll (HNLC) regions. *Mar. Ecol. Prog. Ser.*, **252**, 15–33.

Franck, V. M., Smith, G. J., Bruland, K. W. and Brzezinski, M. A. (2005) Comparison of size-dependent carbon, nitrate, and silicic acid uptake rates in high and low iron waters. *Limnol. Oceanogr.*, **50**, 825–838.

Fraústo Da Silva, J. J. R. and Williams, R. J. P. (2001) *The Biological Chemistry of the Elements: The Inorganic Chemistry of Life*. Oxford University Press, New York.

Gorokhova, E. (2003) Relationships between nucleic acid levels and egg production rates in *Acartia bifilosa*: implications for growth assessment of copepods *in situ*. *Mar. Ecol. Prog Ser.*, **262**, 163–172.

Hansen, B. W., Marker, T., Andreassen, P., Arashkewich, E., Carlotti, F., Lindeque, P., Tande, K. S. and Wagner, M. (2003) Differences in life-cycle traits of *Calanus finmarchicus* originating from 60 degrees N and 69 degrees N, when reared in mesocosms at 69 degrees N. *Mar. Biol.*, **142**, 877–893.

Hessen, D. O. (1992) Nutrient element limitation of zooplankton production. *Am. Nat.*, **140**, 799–814.

Hessen, D. O. and Persson, J. (2009) Genome size as a determinant of growth and life-history traits in crustaceans. *Biol. J. Linn. Soc.*, **98**, 393–399.

Hirst, A. G. and Bunker, A. J. (2003) Growth of marine planktonic copepods: global rates and patterns in relation to chlorophyll a, temperature, and body weight. *Limnol. Oceanogr.*, **48**, 1988–2010.

Ikeda, T., Sano, F., Yamaguchi, A. and Matsuishi, T. (2007) RNA:DNA ratios of calanoid copepods from the epipelagic through abyssopelagic zones of the North Pacific Ocean. *Aquat. Biol.*, **1**, 99–108.

Jones, R. H., Flynn, K. J. and Anderson, T. R. (2002) Effect of food quality on carbon and nitrogen growth efficiency in the copepod *Acartia tonsa*. *Mar. Ecol. Prog Ser.*, **235**, 147–156.

Kiørboe, T. (1989) Phytoplankton growth rate and nitrogen content—implications for feeding and fecundity in a herbivorous copepod. *Mar. Ecol. Prog. Ser.*, **55**, 229–234.

Kuijper, L. D. J., Anderson, T. R. and Kooijman, S. (2004) C and N gross growth efficiencies of copepod egg production studied using a Dynamic Energy Budget model. *J. Plankton Res.*, **26**, 213–226.

Landry, M. R., De Verneil, A., Goes, J. I. and Moffett, J. W. (2016a) Plankton dynamics and biogeochemical fluxes in the Costa Rica Dome: introduction to the CRD Flux and Zinc Experiments. *J. Plankton Res.*, **38**, 167–182.

Landry, M. R., Selph, K. E., Décima, M., Gutiérrez-Rodríguez, A., Stukel, M. R., Taylor, A. G. and Pasulka, A. L. (2016b) Phytoplankton production and grazing balances in the Costa Rica Dome. *J. Plankton Res.*, **38**, 366–379.

Marchetti, A., Parker, M. S., Moccia, L. P., Lin, E. O., Arrieta, A. L., Ribalet, F., Murphy, M. E. P., Maldonado, M. T. *et al.* (2009) Ferritin is used for iron storage in bloom-forming marine pennate diatoms. *Nature*, **457**, 467–470.

Malzahn, A. M. and Boersma, M. (2012) Effects of poor food quality on copepod growth are dose dependent and non-reversible. *Oikos*, **121**, 1408–1416.

Malzahn, A. M., Hantzsche, F., Schoo, K. L., Boersma, M. and Aberle, N. (2010) Differential effects of nutrient-limited primary production on primary, secondary or tertiary consumers. *Oecologia*, **162**, 35–48.

Minas, H. J., Minas, M. and Packard, T. T. (1986) Productivity in upwelling areas deduced from hydrographic and chemical fields. *Limnol. Oceanogr.*, **31**, 1182–1206.

Moore, J. K., Doney, S. C. and Lindsay, K. (2004) Upper ocean ecosystem dynamics and iron cycling in a global three-dimensional model. *Global Biogeochem. Cycles*, **18**, GB4028.

Morel, F. M. M., Reinfelder, J. R., Roberts, S. B., Chamberlain, C. P., Lee, J. G. and Yee, D. (1994) Zinc and carbon co-limitation of marine phytoplankton. *Nature*, **369**, 740–742.

Nunez-Milland, D. R., Baines, S. B., Vogt, S. and Twining, B. S. (2010) Quantification of phosphorus in single cells using synchrotron X-ray fluorescence. *J. Synchr. Rad.*, **17**, 560–566.

Oliveira, L. and Antia, N. J. (1986) Nickel ion requirements for autotrophic growth of several marine microalgae with urea serving as nitrogen source. *Can. J. Fish. Aquat. Sci.*, **43**, 2427–2433.

Price, N. M. and Morel, F. M. M. (1991) Colimitation of phytoplankton growth by nickel and nitrogen. *Limnol. Oceanogr.*, **36**, 1071–1077.

Raven, J. A., Evans, M. C. W. and Korb, R. E. (1999) The role of trace metals in photosynthetic electron transport in O_2-evolving organisms. *Photosynth. Res.*, **60**, 111–149.

Reinfelder, J. R. and Fisher, N. S. (1991) The assimilation of elements ingested by marine copepods. *Science*, **251**, 794–796.

Saito, M. A., Rocap, G. and Moffett, J. W. (2005) Production of cobalt binding ligands in a *Synechococcus* feature at the Costa Rica upwelling dome. *Limnol. Oceanogr.*, **50**, 279–290.

Schmidt, M. A., Zhang, Y. H. and Hutchins, D. A. (1999) Assimilation of Fe and carbon by marine copepods from Fe-limited and Fe-replete diatom prey. *J. Plankton Res.*, **21**, 1753–1764.

Selph, K. A., Landry, M. R., Taylor, A. G., Gutiérrez-Rodríguez, A., Stukel, M. R., Wokuluk, J. and Pasulka, A. (2016) Phytoplankton production and taxon-specific growth rates in the Costa Rica Dome. *J. Plankton Res.*, **38**, 199–215.

Speekmann, C. L., Nunez, B. S. and Buskey, E. J. (2007) Measuring RNA:DNA ratios in individual. *Acartia tonsa* (Copepoda). *Mar. Biol.*, **151**, 759–766.

Sterner, R. W. and Elser, J. J. (2002) *Ecological Stoichiometry: The Biology of Elements from Molecules to the Biosphere*. Princeton University Press, Princeton, NJ.

Sterner, R. W. and Hessen, D. O. (1994) Algal nutrient limitation and the nutrition of aquatic herbivores. *Annu. Rev. Ecol. Syst.*, **25**, 1–29.

Strzepek, R. F. and Harrison, P. J. (2004) Photosynthetic architecture differs in coastal and oceanic diatoms. *Nature*, **431**, 689–692.

Sunda, W. G. and Huntsman, S. A. (1992) Feedback interactions between zinc and phytoplankton in seawater. *Limnol. Oceanogr.*, **37**, 25–40.

Sunda, W. G. and Huntsman, S. A. (1997) Interrelated influence of iron, light and cell size on marine phytoplankton growth. *Nature*, **390**, 389–392.

Sunda, W., Kieber, D. J., Kiene, R. P. and Huntsman, S. (2002) An antioxidant function for DMSP and DMS in marine algae. *Nature*, **418**, 317–320.

Taylor, A. G., Landry, M. R., Freibott, A., Selph, K. E. and Gutiérrez-Rodríguez, A. (2016) Patterns of microbial community biomass, composition and HPLC diagnostic pigments in the Costa Rica upwelling dome. *J. Plankton Res.*, **38**, 183–198.

Tukey, J. (1949) Comparing individual means in the analysis of variance. *Biometrics*, **5**, 99–114.

Twining, B. S. and Baines, S. B. (2013) The trace metal composition of marine phytoplankton. *Annu. Rev. Mar. Sci*, **5**, 191–215.

Twining, B. S., Baines, S. B., Bozard, J. B., Vogt, S., Walker, E. A. and Nelson, D. M. (2011) Metal quotas of plankton in the equatorial Pacific Ocean. *Deep-Sea Res. II*, **58**, 325–341.

Twining, B. S., Baines, S. B. and Fisher, N. S. (2004) Element stoichiometries of individual plankton cells collected during the Southern Ocean Iron Experiment (SOFeX). *Limnol. Oceanogr.*, **49**, 2115–2128.

Twining, B. S., Baines, S. B., Fisher, N. S., Maser, J., Vogt, S., Jacobsen, C., Tovar-Sanchez, A. and Sanudo-Wilhelmy, S. A. (2003) Quantifying trace elements in individual aquatic protist cells with a synchrotron X-ray fluorescence microprobe. *Anal. Chem.*, **75**, 3806–3816.

Twining, B. S., Baines, S. B., Vogt, S. and Nelson, D. M. (2012) Role of diatoms in nickel biogeochemistry in the ocean. *Global Biogeochem. Cycles*, **26**, GB4001.

Twining, B. S., Nunez-Milland, D., Vogt, S., Johnson, R. S. and Sedwick, P. N. (2010) Variations in *Synechococcus* cell quotas of phosphorus, sulfur, manganese, iron, nickel, and zinc within mesoscale eddies in the Sargasso Sea. *Limnol. Oceanogr.*, **55**, 492–506.

Villar-Argaiz, M. and Sterner, R. W. (2002) Life history bottlenecks in *Diaptomus clavipes* induced by phosphorus-limited algae. *Limnol. Oceanogr.*, **47**, 1229–1233.

Vogt, S. (2003) MAPS: a set of software tools for analysis and visualization of 3D X-ray fluorescence data sets. *J. Phys. IV*, **104**, 635–638.

Wolfe-Simon, F., Grzebyk, D., Schofield, O. and Falkowski, P. G. (2005) The role and evolution of superoxide dismutases in algae. *J. Phycol.*, **41**, 453–465.